

REMOTE ESTIMATION OF TOTAL SUSPENDED SOLID (TSS) TRANSPORT AFFECTED BY TIDAL BORE “BONO” OF KAMPAR BIG RIVER ESTUARY USING LANDSAT 8 OLI IMAGERY

Ulung Jantama Wisna^{*}, Ruzana Dhiauddin, and Gunardi Kusumah

Research Institute for Coastal Resources and Vulnerability, KKP. Padang, Indonesia

^{*}Correspondence author: ulungjantama@gmail.com

Received: September 2016

Accepted: May 2017

ABSTRACT

The Kampar River estuary has a unique tidal bore, namely Bono. A tidal bore is a natural phenomenon caused by the tidal flow which meet the flow of the river. Tidal bore “Bono” has an impact on the transport of suspended particles which is pretty much along the Kampar River. The purpose of this study is to determine the estimated concentration of total suspended solid in the river as the result of the transport by Bono in Kampar River estuary by Landsat 8 OLI. The primary data are Landsat 8 OLI sensor – on Path 126 and Row 60, recording date was on 23-04-2016, which was analyzed spatially – and TSS *in situ*. The secondary data are tide forecasting data and topographical map of Indonesia. Distribution of total suspended solid indicates sediment transport and its distribution by TSS values ranged between 10-150 mg/L and TSS *in situ* value ranged between 42-241 mg/L. Tidal range ranged from 0.78 to 4.2 m and current velocity ranged from 0-0.9 m/s, which generate tidal bore extending from the mouth to the river body, resulting in suspended particle transport along the river. TSS concentration is higher in the river estuary.

Keywords: GIS, Kampar River, Landsat 8 imagery, Tidal Bore, Total Suspended solid

INTRODUCTION

Bono is a natural phenomenon caused by the propagation of tidal current from the estuary. Estuary shape is divergent, which is affected the higher speed of Bono and is supported by the convergence of two kinds of currents; the upstream flow and the tidal flow from the estuary. Bono waves included in the category of Tidal Bore which was defined by Yulistyanto (2009) the hydrodynamic phenomena associated with the mass movement in the estuary water, where the tidal wave propagates to upstream with the destructive force.

The emergence of Bono waves has significant impacts on the system of the estuary. The impacts are sand transport and deposition which occurred around Muda Island and Mendol Island

(Yulistyanto, 2009). Mixing in the riverbeds is caused by the hydraulic jump flow of tidal bore (Chanson, 2008). The high sediment transport is also caused by mixing mechanism which occurs when the Bono propagates along the Kampar River so that the suspension of sediment constantly occurs and causes the high turbidity levels in the estuary (Riau Research Agency, 2005).

In some areas along the Kampar River, there are sand mining areas explored by the public. It has positive and negative impacts on social and environmental aspects. The region that became the center of sand mining is Teluk Meranti and Kuala Kampar Village with a total mining area reached 508.17 ha (Department of Energy and Mineral Resources District. Pelalawan, 2009). Sand mining which causes changes to the morphology

of the river and shipping lanes and the presence of Bono, which contribute significantly to the sediment transport mechanism.

Distribution of suspended materials concentration in the Kampar River can be calculated by a Landsat 8 algorithm. Landsat 8 carries two separate sensors, namely the Operational Land Imager (OLI) and the Thermal Infrared Radiometer Suite (TIRS) (Pahlevan and Schott, 2011) that image the earth surface throughout the visible and thermal portions of the spectrum.

Compared to earlier version of Landsat sensors, the OLI has enhanced features, including its 12 bit radiometric resolution and the addition of a band centered at 443 nm. The improvement of data quality/quantity expands the existing applications of Landsat imagery in aquatic sciences from the retrieval of biogeochemical properties, including total suspended solids (TSS) (Pahlevan *et al.*, 2014).

Research on the phenomenon of tidal bore “Bono” in Indonesia is still rare and none of that previous studies has in depth study about Bono phenomenon, its causes, and effects on the Kampar River waters and estuaries environment. The purpose of this study was to determine the estimated concentration of TSS in the Kampar River transported by tidal bore Bono in Riau Kampar River estuary using Landsat 8 OLI.

MATERIALS AND METHODS

The material used in this study included primary data and secondary data. The primary data were TSS *in situ* and Landsat 8 OLI of Kampar River (Pelalawan Regency) at Path 126 and Row 60, recorded on April 23, 2016. The recording was taken from USGS web pages <http://earthexplorer.usgs.gov/>. Table 1 shows that the image recording time is in accordance with the sampling time TSS *in situ*, which were taken in the same tidal condition (Figure 1). The secondary data consisted of digital topographical map of Indonesia used for cross section layout map and NAOtide forecasting used for determination of field data collection time according to high tide to low tide.

Table 1. Landsat 8 image specification

No	Dataset attribute	Attribute value
1	Landsat scene identifier	LC1260602016114LGN00
2	Bias parameter file name OLI	LO8BPF20160423030011_20160423034201.01
3	Day/night	Day
4	Date acquired	2016/04/23
5	Start time (GMT+7)	10:22:28
6	Stop time (GMT+7)	10:23:00

Radiometric correction function was used to equalize the solar conditions in each region/pixel in the image to get the reflectance value by changing the value of Digital Number (DN) into the reflectance value. This was achieved by algorithm formula according to USGS (2016) as follows:

$$\rho\lambda' = M\rho * Q_{cal} + A\rho$$

where:

$\rho\lambda'$ = TOA (Top of Atmospheric) planetary reflectance, without correction for the solar angle.

$M\rho$ = Band-specific multiplicative rescaling factor from the metadata.

$A\rho$ = Band-specific additive rescaling factor from the metadata.

Q_{cal} = Quantized and calibrated standard product pixel values (DN).

TOA reflectance was corrected based on the sun angle following formula as follow:

$$\rho\lambda = \rho\lambda' / \text{Sin}(\theta_{SE})$$

where:

$\rho\lambda$ = TOA planetary reflectance

θ_{SE} = Local sun elevation angle

The clouds were masked out of the image. Hence, in the calculation of TSS, land and clouds were not included in the calculation. The masking process was done by employing following formula:

$$\text{If } (i2/i1) < 1.3 \text{ then null else } i2$$

where:

$$i2 = \text{band 4 (0.64 - 0.67 } \mu\text{m)}$$

$$i1 = \text{band 5 (0.84 - 0.89 } \mu\text{m)}$$

(Simbolon *et al.*, 2015)

The use of the above equation is in conjunction with TSS algorithm by Budhiman (2004) that has been implemented by Putra *et al.* (2014) in their work as follows:

$$\text{TSS (mg/L)} = 8.1429 \times \text{EXP}^{(23.704 * \text{red band})}$$

Where: red band = band 4

In the present study, the calculation of TSS only used reflectance ($\rho\lambda$) from the red band, combined with the value of the separation of land and sea. The formula was formulated as follows:

If $(i2/i1) < 1.3$ then null else (TSS)

Water sampling was done during ebb tide conditions (Figure 1) based on tide forecasting using NAOtide at longitude 103.22603 and latitude 0.50354. This aimed to achieve the same conditions to establish the comparison of the obtained TSS and water quality parameters. Data were collected on the April, 26th 2016 at 07:00 - 11:00 am. At the tidal condition, the water in Kampar River estuary waters are high tide towards low tide.

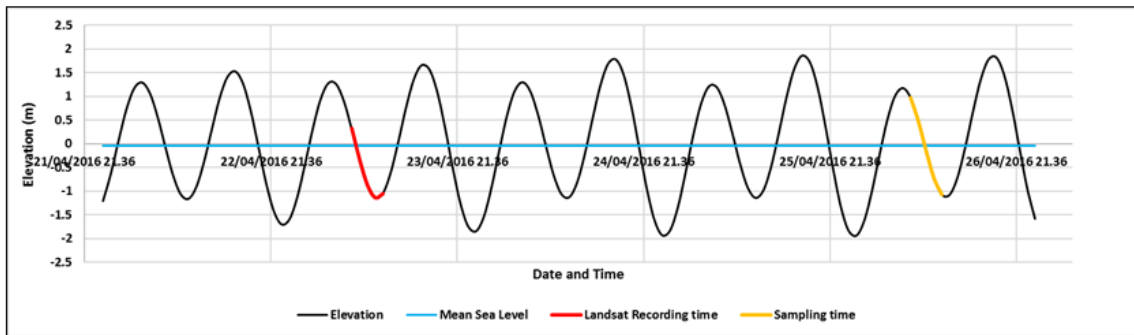


Figure 1. Sampling time based on Tide forecasting by NAOtide

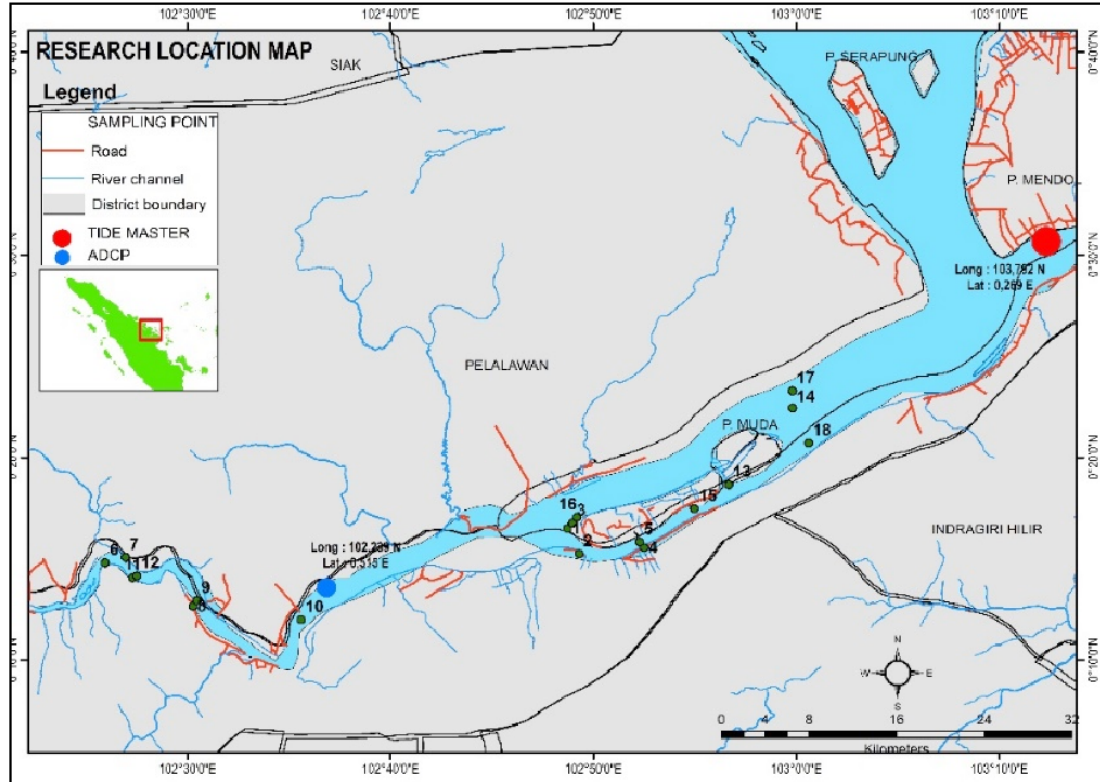


Figure 2. Research location of Kampar River estuary

TSS sample analysis was done using *gravimetric methods* SNI 06-6989.3-2004. About 100mL of water samples were collected, gently shaken and filtered using a vacuum pump and Whatman filter paper with 0.45 μm pore size. Filters were then weighed and TSS concentrations were calculated using the formula as follow:

$$C_{si} = \frac{(G_2 - G_1) \times 1000}{V} \text{ mg/L}$$

where:

C_{si} = Level of sediment suspensions mg/L

G₂ = Weight of filter paper and precipitate after heated (mg)

G₁ = Weight of filter paper blank (mg)

V = Volume of the filtered water (mL)

To evaluate the TSS image processing result, it must be compared with field measurement TSS data (Volpe *et al.*, 2011), applying RMSE (Root Mean Square Error) formula as follows:

$$RMSE = \sqrt{\frac{1}{N} \sum_{i=1}^N (x_i - y_i)^2}$$

where:

N = The number of total data

x_i, x_i = Image processing data result

y_i, y_i = Field measurement data result

Measurement of tide was done using *Tide gauge Valeport*, from April 23 to May 23 of 2016 in the South of Mendol Island (Figure 2). The tidal data calculation includes tidal range and analysis of *Indian Spring Low Water* (ISLW) (Adibrata, 2007). Tidal range was obtained by calculating the difference between high tide and low tide, while the value of amplitude and phase delay was analyzed using *Ergtide software* combined with admiralty analysis for 29 days tide data.

Measurement of current with the principle *Euler* method was done at one point location using the ADCP (Acoustic Doppler Current Profiler) *Aquadop Profiler NORTEK* (Table 2). This avoids the disturbance *i.e.* the activities of fishermen and vessel traffic (Wisha *et al.*, 2015). The ADCP was deployed in the Tanjung Tersenduk-senduk area (Figure 2). The current measurements during 24 hours data was carried out to represent the speed and direction of currents and the surface elevation (Wisha *et al.*, 2016b).

Table 2. Acoustic Doppler Current Profiler Specification

Acoustic frequency	0.6 MHz
Max profile range	30 - 40 m
Cell size	1 - 4 m
Minimum blanking	0.5 m
Max cell	128
Velocity range	± 10 m/s
Accuracy	1% of measured value ± 0.5 cm/s
Max sampling range	1 Hz

RESULT AND DISCUSSION

OLI image processing results showed that TSS concentrations ranged from 10 to 150 mg/L and TSS concentration value of the *in situ* station ranged between 63 – 141 mg/L (Figure 3). TSS value varied from the estuary to upstream. According to Rosyadi *et al.* (2009) the value of TSS in Kampar estuary ranged from 86.33 to 115.96 mg/L, Rozali *et al.* (2016) also stated that the concentration of TSS in Kampar River estuary ranged between 70-110 mg/L during low tide towards high tide and 50-150 mg/L during high tide towards low tide. The variation of these findings is consistent with the study carried out by the Ministry of Environment and Forestry (2014) reported that the annual concentration from 2010 to 2014 of TSS in Kampar River was volatile and unstable (Table 3).

Table 3. TSS concentration in the Kampar River every year

No	Year	TSS Concentration (mg/L)
1	2010	83.12
2	2011	96.28
3	2012	51.89
4	2013	55.10
5	2014	36.89

(Source: Ministry of Environment and Forestry, 2014)

TSS concentration at high tide towards low tide condition is higher due to the existing intake of suspended substances from Malacca Strait transported by the tidal current. When the Bono propagates, it mixed the sediment and particles in the bottom of the river. Bono propagation brings the large tidal energy and destructively causes the erosion in the estuary area. According to Furgerot *et al.*, (2013), the turbulence due to tidal bore

propagation is directly related to enhanced TSS concentration in the estuary.

The transport of sediment due to Bono propagation occurring along the Kampar River also affects sedimentation in the upstream area (Yulistyanto, 2009). The unstable sedimentation that changes in each season affects the stream channel in some part of the upstream.

From the results of image processing, some samples were chosen to find a more detailed of TSS concentration that divided into 6; **A, B, C, D, E** and **F** (Figure 3). All those locations have the same coordinates with the measurement location TSS *in situ* (Table 4).

The lowest TSS concentration was at station 14 and the highest was station 18 located in the Kampar estuary. According to Donnelly and Chanson (2002) high suspension of the organic/inorganic substances increased in the estuary as a result of the turbulence and mixing by a hydraulic jump of tidal bore. These conditions lead to the increasing turbidity enhancement in the estuary.

The error value of TSS concentration obtained from the comparison between OLI imagery and field measurements was 7.98%. Figure 4 shows that the difference in results verified that TSS concentration is different at each observation stations.

The distributions of suspended particles stirred by the tidal bore is a dominant factor to change the turbidity. Yulistyanto (2009) reported that Bono propagations reach 60km upstream. During the propagation, the Bono's energy generates the hydro sedimentary processes which trigger the erosion and sedimentation events along the river (Chanson, 2001).

The high TSS in the river generates the environmental pollution and disrupts the biogeochemical processes. According to Rosyadi *et al.*, (2009), TSS is a major factor affecting the decreasing of phytoplankton photosynthesis intensity and indirectly influences the other biota in the food chain.

Tidal bore Bono causes the upstream turbidity level enhanced due to the transported suspended particles from the river mouth. This condition also affects the water quality parameters inside the river as a tidal bore, activities directly affect

the distribution of many chemical compounds and change the level of the standard quality of environment (Chanson, 2011).

Table 4. TSS remote estimation from OLI sensor imagery

Code	Station	TSS Concentration (mg/L)
A	14	71.30
	17	76.39
	18	148.87
B	13	98.73
	15	96.56
C	1	130.58
	2	99.97
	3	129.86
	4	97.55
	5	95.73
	16	120.65
D	10	74.81
E	8	137.60
	9	132.84
F	6	121.12
	7	125.45
	11	86.75
	12	88.93

Table 5. Descriptive statistics water quality parameters

Parameter	Min	Max	Mean	SD
Turbidity (NTU)	2111.40	3760.40	2745.53	365.38
TDS (g/L)	0.00	7.40	1.65	2.18
DO (mg/L)	4.39	6.71	5.25	0.54
Temperature (°C)	30.30	32.70	30.92	0.69

The water quality data were obtained by field measurement at the same time and the same point of TSS *in situ* (Table 5). The value of turbidity ranged from 2111.40 to 3760.40 NTU, with an average of 2745.54 ± 365.38 . Turbidity is closely related to the levels of suspended substances. The turbidity value in the present study was quite high. It indicates that the suspended particle concentration was also high. It will reduce the visibility level in the waters, which is finally will inhibit the photosynthesis activities.

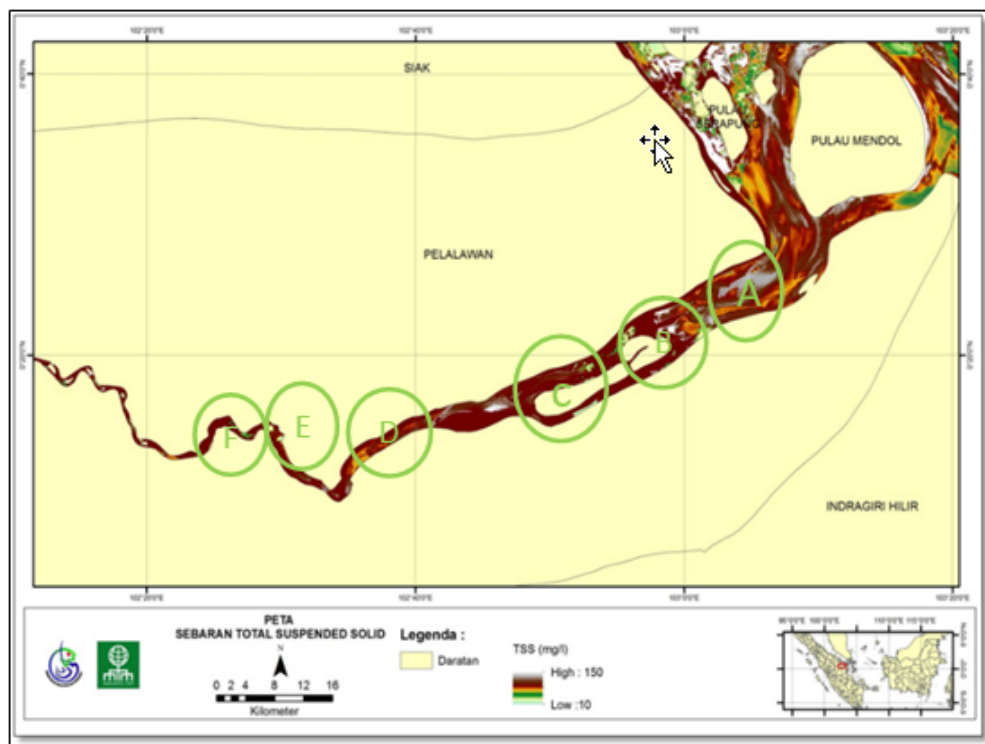


Figure 3. Processing result of TSS distribution using OLI sensor imagery

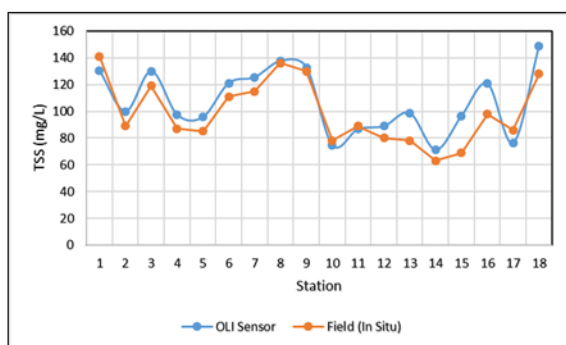


Figure 4. TSS comparison between analyze from OLI sensor and field data

Total dissolved solid (TDS) ranged from 0 to 7.40 g/L (Tabel 5). The value of TDS is associated with the level of solid content in the water, dissolved solids and suspended solids which is a parameter for determining the total solids. This can be organics and inorganics which indirectly influence the biota inside the river especially for phytoplankton photosynthesis. According to Wisna *et al.*, (2016a), the abundance of phytoplankton is inversely proportional to solids content, turbidity, and suspended materials.

Dissolved Oxygen (DO) is an unstable parameter. The increasing value of TSS and

turbidity will inhibit the process of photosynthesis by autotroph organisms and decrease the dissolution of oxygen in the water. It will lead to anoxic conditions in the water (Clingan and Norton, 1987). In the present study, the DO value ranged from 4.39 to 6.71 mg/L with an average value in all sampling stations of 5.25 ± 0.53 mg/L (Table 5). DO value is categorized under normal conditions.

Temperature is a physical factor that affects the speed of the suspended particles settling process (Hala *et al.*, 2013), the temperature ranged from 30.30 to 32.70°C with an average temperature value of 30.92 ± 0.69 °C.

Tidal change with a range up to 4 m is necessary for a tidal bore (Chanson, 2009). The tidal energy sourced from Malacca Strait, which generated a high range of tidal elevation change. It causes a wave propagation which triggers a destructive force. The tidal wave (Bono) affects the instability of the bed morphology which depends on the seasons, tidal conditions and wind directions. Propagation of tidal bore is a major factor in the mechanism of water mass transport along the river (Baschek *et al.*, 2001).

Table 6 shows that the type of tidal in the estuary of Kampar River is a mixed tide prevailing semidiurnal, with a tidal range is 4.20 m on spring tide conditions and 2.50 m on neap tide condition. The maximum tidal elevation for one tidal cycle is ranged from 0.49 to 4.69 m, which each constituent parameter represents: Z_0 = Surface elevation under the lowest ebb

LAT = Lowest astronomical tides
 HAT = Highest astronomical tides
 MHHWS = Mean highest of high waters spring
 MLHWN = Mean lowest of high water neap
 MLLWS = Mean lowest of low water spring
 MLLWN = Mean lowest of low water neap

In the Muda Island, the pressure convergence of tidal flow and river flow triggers a formation of hydraulic jump off a tidal bore which forms a large energy. The energy decreases significantly in Teluk Meranti village (downstream area). According to Chanson (2009) the height of hydraulic jump off a tidal bore depends on streamflow and tidal energy.

At the time of tidal bore propagation, the turbulence for bottom sediments is stirred by a

hydraulic jump off the tidal bore (Chanson *et al.*, 2010) which are transported and settled in the upstream area (Chanson, 2004). Bed erosion could possibly take place beneath each wave crest. The eroded material is advected in the wave motion behind the first wave crest and the turbulence become stronger (Koch and Chanson, 2008).

The results of ADCP measurements (Figure 5) indicate two current characteristics at the time of the afternoon Bono event (red circle) and the night Bono event (black circle). In the afternoon event, the water level is about 3.40 m. The current direction changed significantly but the current speed decrease at the same time of Bono occurrence, about 0.20 m/s.

In contrast, the water level during the night is 4.10 m, while current direction changed is almost 250° and the velocity reaches 0.90 m/s. According to our results, the speed of the tidal bore ranged between 0.20-0.9 m/s that are slightly different from the results of Garonne River (about 0.30-1.00 m/s) reported by Chanson *et al.* (2010). According to Furgerot *et al.* (2013), the speed of the tidal bore depends on the tidal elevation

Table 6. Tidal analysis result for tidal constituent parameters

Z_0	LAT	HAT	MHHWS	MLHWN	MLLWN	MLLWS	F	Tidal range	
0.49 m	0.49 m	4.69 m	3.22 m	2.74 m	2.44 m	1.96 m	0.43	2.50 m	4.20 m
							Mixed tide prevailing semidiurnal	Neap	Spring

range, which forms a harmonic oscillation along the river. It becomes the major factor which triggers the suspended particles distribution.

In addition, the use of uncorrected data atmospherically will affect to the result of suspended particle concentrations. It can be higher/lower than the real concentration (There is a bit of error inside) due to the influence of scattering and radiation absorption.

CONCLUSION

TSS concentration of remote estimation OLI imagery is not much different from the measurement results of TSS *in situ*. The range of TSS value is high enough and also affects the change in a value of some physical and chemical parameters of Kampar estuary. Wave propagation Bono evokes particles stirred in the bottom of the river mouth and brought it to the upstream, which the oscillation bore occurred 2 times in one day.

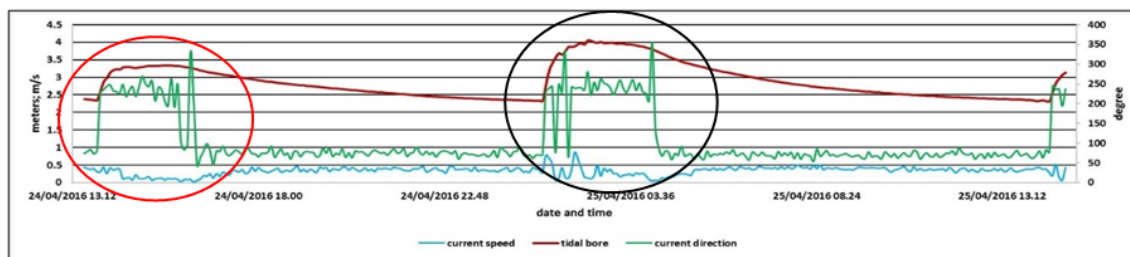


Figure 5. Kampar Estuary flow dynamics measured by ADCP

Water elevation and current speed are different between the 2 events of Bono propagation and the suspended particles transport might also be different at each event.

The use of Landsat imagery to estimate the TSS concentrations can also be applied to estimate the sedimentation area. The algorithm that is used in the present study is quite precise in describing the impact of Bono waves on sedimentation and turbulence in Kampar River. However, it could have considerable errors for other images with the larger water areas.

This study can be useful as a basis for the assessment of the current environmental conditions of Kampar River for the local government by which sand mining activities in the Kampar river can be potentially controlled.

ACKNOWLEDGEMENT

Acknowledgment for Research Institute of Coastal Resources and Vulnerability (LPSDKP) on DIPA 2016 research budget in Kampar-Riau, for CV. Mangrove Map and for all those who have assisted in the completion of this scientific paper.

REFERENCES

Adibrata, S. (2007). Tidal Analysis in Karampuang Island, West Sulawesi Province. *Journal Akuatik*. 1(1):1-6.

Baschek, B., Send, U., Lafuente, J.G. and Candela, J. (2001). Transport Estimates in the Strait of Gibraltar with a Tidal Inverse Model. *J. Geophys. Res.* 106 (c12): 31033-31044. Doi: 10.1029/2000JC000458.

Chanson, H. (2001). *Flow Field in a Tidal Bore: A physical Model*. Proc. 29th IAHR Congress, Beijing, Theme E, Tsinghua University, Beijing, pp: 365-373.

Chanson, H. (2004). *Mixing and Dispersion Role of Tidal bores*. Fluvial, Environmental and Coastal Developments in Hydraulic Engineering - Mossa, Yasuda and Chanson (eds), Taylor and Francis Group. London. pp: 223-232.

Chanson, H. (2008). *Turbulence in Positive Surges and Tidal Bores, Effects of Bed Roughness and Adverse Bed Slopes*. Report CH68/08. Division of Civil Engineering. The University of Queensland. St Lucia QLD. 107 pp.

Chanson, H. (2009). Environmental, ecological and Cultural Impacts of Tidal Bores, Benaks, Bonos, and Burros. IWEH, International Workshop on *Environmental Hydraulics Theoretical, Experimental and Computational Solutions*. Valencia, 29th, 30th, October 2009.

Chanson, H., Lubin, P., Simon, B. and Reungoat, D. (2010). Turbulence and Sediment Processes in the Tidal Bore of the Garonne River: First Observations. *Hydraulic Model Report CH79/10*. The university of Queensland. Australia.

Chanson, H. (2011). Current Knowledge in Tidal Bores and Their Environmental, Ecological and Cultural Impacts. *Environ. Fluid. Mech.* 11: 77-98. Doi: 10.1007/s10652-009-9160-5.

Clingan, T., Norton, M.G. (1987). *Wastes in Marine Environment*. Congress of the United States. Office of Technology Assesment. Washington.

Department of Energy and Mineral Resources District. Pelalawan. (2009). Laporan Akhir Kajian Inventarisasi Potensi Sumber Daya Alam di Kabupaten Pelalawan tahun 2009, Pelalawan, Riau.

Donnelly, C. and Chanson, H. (2002). Environmental Impact of Tidal Bores in Tropical Rivers. Proc. 5th International

- River Management Symposium, Brisbane, Australia, September 2002.
- Furgerot, L., Mouaze, D., Tessier, B. and Haquin, S. (2013). Suspended Sediment Concentration in Relation to the Passage of a Tidal Bore (See River Estuary, Mont Saint Michel Bay, NW France). *Coastal Dynamics Conference* in January 2013. France.
- Hala, Y., Syahrul, M., Suryanti, E., Taba, P. and Soekamto N. H. (2013). Biosorption of Zn^{2+} And Cd^{2+} in A Two – Metal System By NannoChloropsis Salina. *Eur.Chem. Bull.* 2(5): 238-24.
- Koch, C. and Chanson, H. (2008). Turbulent Mixing Beneath an Undular Bore Front. *J. Coast. Res.* 24(4): 999-1007. doi: 10.2112/66-0688.1.
- Ministry of Environment and Forestry. (2014). Ministry of Environment and Forestry Statistics 2014. Centre of Data and Information KLHK. Jakarta.
- Pahlevan, N. and Schott, J. R. (2011). Investigating the Potential of the Operational Land Imager (OLI) for Monitoring Case II Waters Using a Look-Up-Table Approach. *Pecora 18-Forty Years of Earth Observation, Understanding a Changing World*, November 14-17, 2011. Herndon, Virginia.
- Pahlevan, Nima, Lee, Z., Wi, J., Schaaf, C. B., Scott, J. R. and Berk, A. (2014). On-Orbit Radiometric Characterization of OLI (Landsat 8) for Application in Aquatic Remote Sensing. *J. Rem. Sen. Env.* 154(1): 272-284. doi: 10.1016/j.rse.2014.08.001.
- Putra, R. M., Semedi, B., Fuad, M. A. Z., and Budhiman, S. (2014). Analisa Sedimen Tersuspensi (Total Suspended Matter) di Perairan Timor Sidoarjo Menggunakan Citra Satelit Landsat dan Spot. *Deteksi Geobiofisik dan Diseminasi Penginderaan Jauh*. Seminar Nasional Penginderaan Jauh 2014.
- Riau Research Agency. (2005). Riau Profile. Retrieved September 22, 2016, 19.43 WIB from <http://balitbang.riau.go.id/7429/go.php?tampilan=profilriau>.
- Rosyadi, R., Syafruddin, N. and Thamrin, T. (2009). The Distribution and Abundance of Macrozoobenthos in Singingi River Riau. *J. Env. Sci.* 3(1): 58-74.
- Rozali, R., Mubarak, M. and Irvina, N. (2016). Patterns of Distribution Total Suspended Solid (TSS) in River Estuary Kampar Pelalawan. *Jurnal Perikanan dan Kelautan.* 3(2): 1-8.
- Simbolon, F., Surbakti, H., and Hartoni. (2015). Distribution Pattern Analysis of Suspended Sediment Using Remote Sensing Technique in Estuary of Banyuasin River. *Maspari Journal.* 7(2):1-10.
- USGS. (2016). Using the USGS Landsat 8 Product (online). U.S. Department of the interior and U.S. Geological survey. USA. http://landsat.usgs.gov/Landsat8_Using_Product.php.
- Volpe, V., Silvestri, S., and Marani, M. (2011). Remote sensing retrieval of suspended sediment concentration in shallow waters. *Remote Sensing of Environment*, 115(1), 44-54. Doi: 10.1016/j.rse.2010.07.013.
- Wisha, U. J., Husrin, S., Prihantono, J. (2015). Hydrodynamics Banten Bay during Transitional Seasons (August-September). *Ilmu Kelautan.* 20(2): 101-112. Doi: 10.14710/ik.ijms.20.2.101-112.
- Wisha, U. J., Yusuf, M., and Maslukah, L. (2016a). Kelimpahan Fitoplankton Dan Konsentrasi Tss Sebagai Indikator Penentu Kondisi Perairan Muara Sungai Porong. *Jurnal Kelautan: Indonesian Journal of Marine Science and Technology*, 9(2), 122-129. Doi: 10.211107/jk.v9i2.1298.
- Wisha U. J., Husrin, S. and Prasetyo, G. S. (2016b). Hydrodynamics of Bontang Seawaters: Its Effects on the Distribution of Water Quality Parameters. *Ilmu Kelautan.* 21(3): 123-134. Doi: 10.14710/ik.ijms.21.3.123-134.
- Yulistyanto, B., (2009). The Phenomenon of Bono Rising Wave in Kampar River Estuary. *Dinamika Teknik Sipil*, 9(1):19-26.